National Aeronautics and Space Administration
Jet Propulsion Laboratory
California Institute of Technology
Pasadena, California

# Mega Urban Changes and Impacts in the Decade of the 2000s

IDS Team: PI: S. V. Nghiem[1]; Co-Is: C. Small[2], M. Z. Jacobson[3], D. Balk[4]; Collaborators: A. Richter[5], K. Gurney[6], P. B. Shepson[7], M. Marcetti[8], A. Sorichettar[9], C. Field[10], D. K. Hall[11], and U. Deichman[12]

[1]JPL, [2]Columbia U., [3]Stanford U., [4]CUNY, [5]Bremen U., [6]Arizona U., [7]Purdue U., [8]Milan U., [9]JRC, [10]Carnegie I., [11]NASA GSFC, and [12]World Bank

**IDS Selected Research**

- **Objective**
  Measure global urban changes and study environmental and socio-economic impacts.
- **Coverage**
  Global in the decades of 2000s.
- **Initial Results**

1. The Beijing Case Study: Book Chapter, Encyclopedia of Remote Sensing, Springer Publisher, on-line Dec. 2012, in print spring-summer 2013.
2. Invited presentation on Mega Urbanization in China at U.S. State Dept., Colglazier attended, Oct. 2012.
3. Provided review comments on the Global Trends 2030, National Intelligence Council, released to Pres. Obama in Dec. 2012.
4. Request from the World Bank for rate of urbanization and rate of pollution in China: High profile interests from WB President Jim Kim and China Premier Li Keqiang, Feb. 2013.

## Addressing Five Science Areas:

1. Can the urban environment be characterized based on physical and measurable parameters such as infrastructures (houses, buildings, factories, etc.) together with high-resolution urban information content (e.g. light/optical data) rather than arbitrary political and administrative units?
2. Can the rate of change in the urban environment be consistently and continuously delineated without spatial and temporal gaps in a decadal timeframe and at the scale relevant to addressing key issues in environmental as well as social science?
3. How does urban change, from mega urbanization like in Asia to stable urban areas, impact the environment through processes involving pollution (e.g., $NO_2$), particulates (e.g., PM10 with size ~10 μm), green-house-gas (GHG) emission ($CO_2$), urban heat island (UHI), urban dome, air quality and health exposure (e.g., smog, ozone), ground water contamination (e.g., nitrate), temperature change, light contamination, and urban-climate interactions?
4. How does urban change affect the socioeconomic spectrum of spatial and structural transformations, including the role of the rural non-farm sector in towns and small cities, rural-urban migration decisions, the dynamics of land markets in peri-urban areas, the degree and nature of specialization in cities of different sizes and at different development stages, and the identification of urban agglomeration benefits and congestion diseconomies?
5. Can mega urban change exacerbate water resource problems (e.g., drought and population dynamics in extreme urbanization) as well as natural and man-made disasters (e.g., extreme urbanization in regions prone to wild fire, flood, tsunami; infrastructure failures, etc.)?

## Satellite Observations:

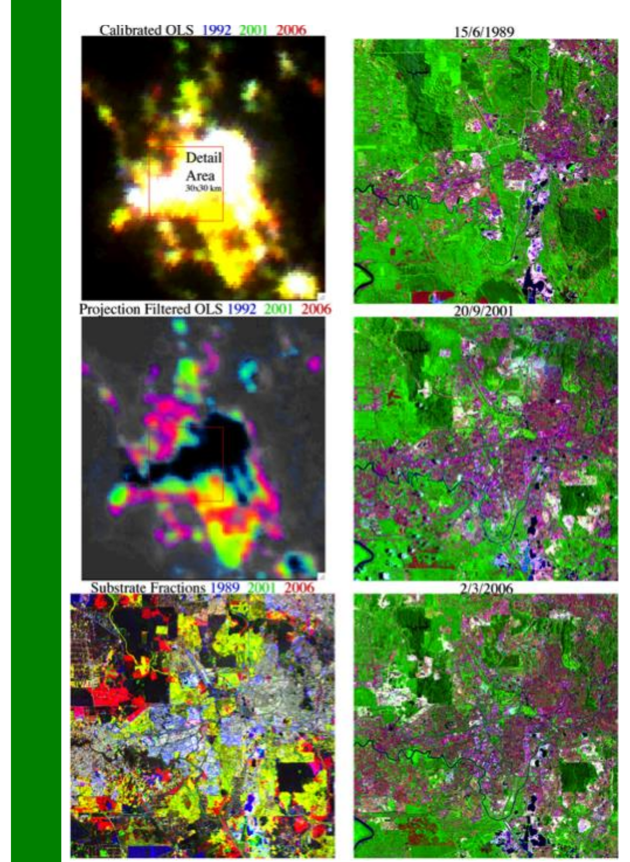

OLS and Landsat Tri-temporal change: Kuala Lumpur, Malaysia

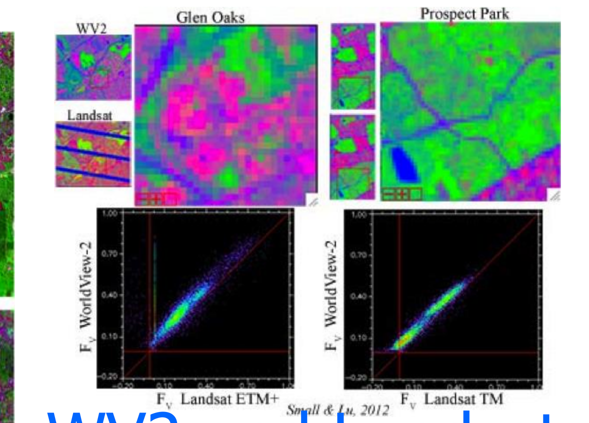

WV2 and Landsat Study of New York

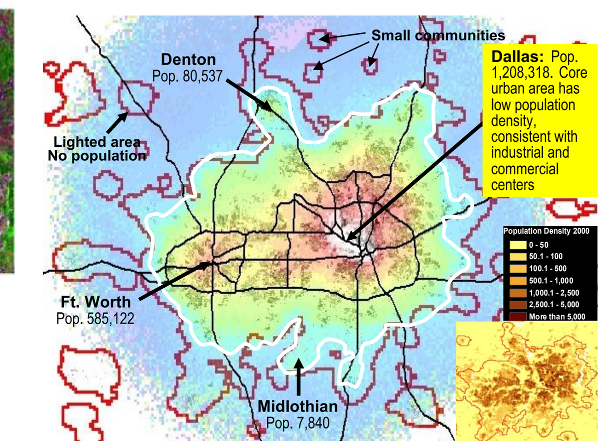

Scatterometer DSM Ft. Worth-Dallas

## Environmental and Demographic Charateristics:

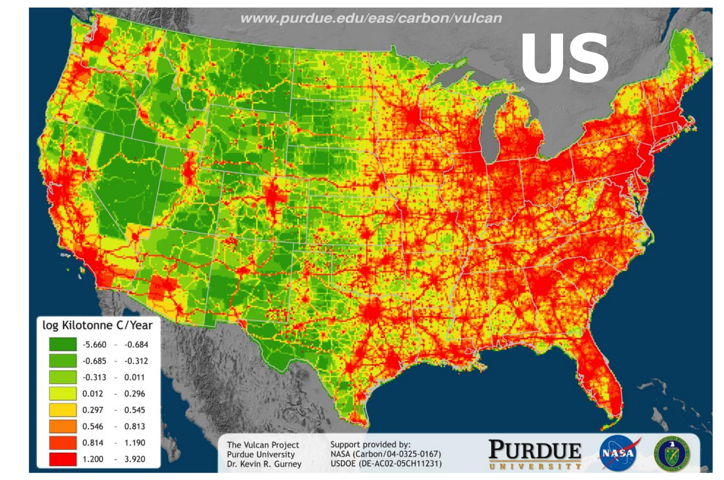


Vulcan: $CO_2$ emission

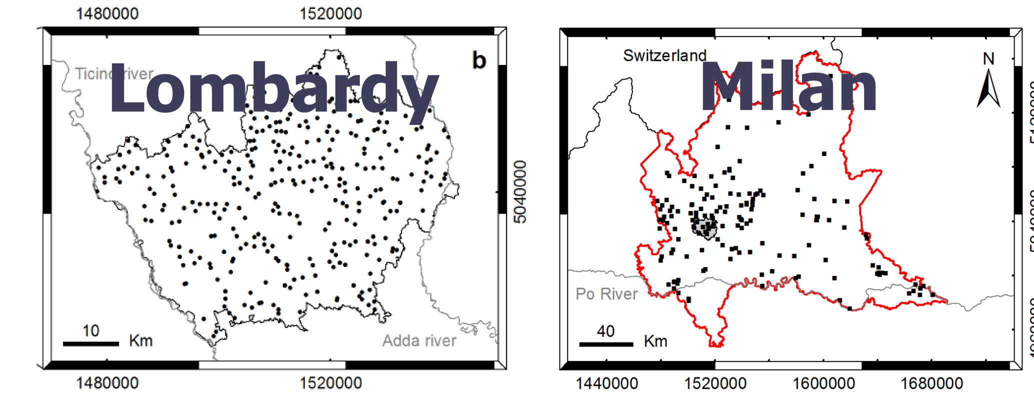


Ground water and air quality sites

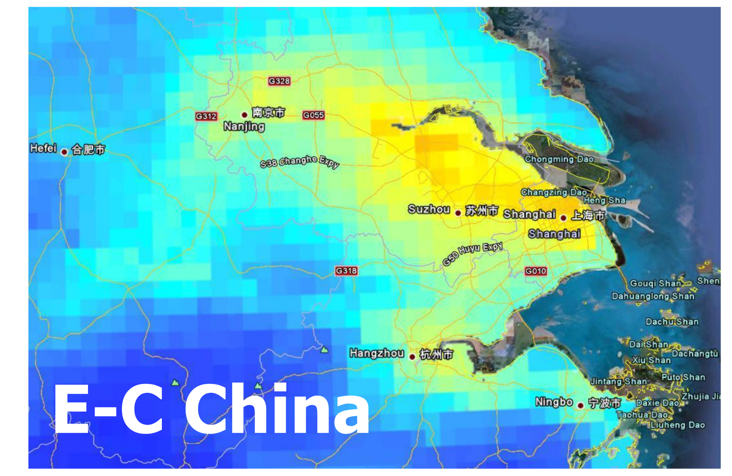


GOME2: $NO_2$ pollution

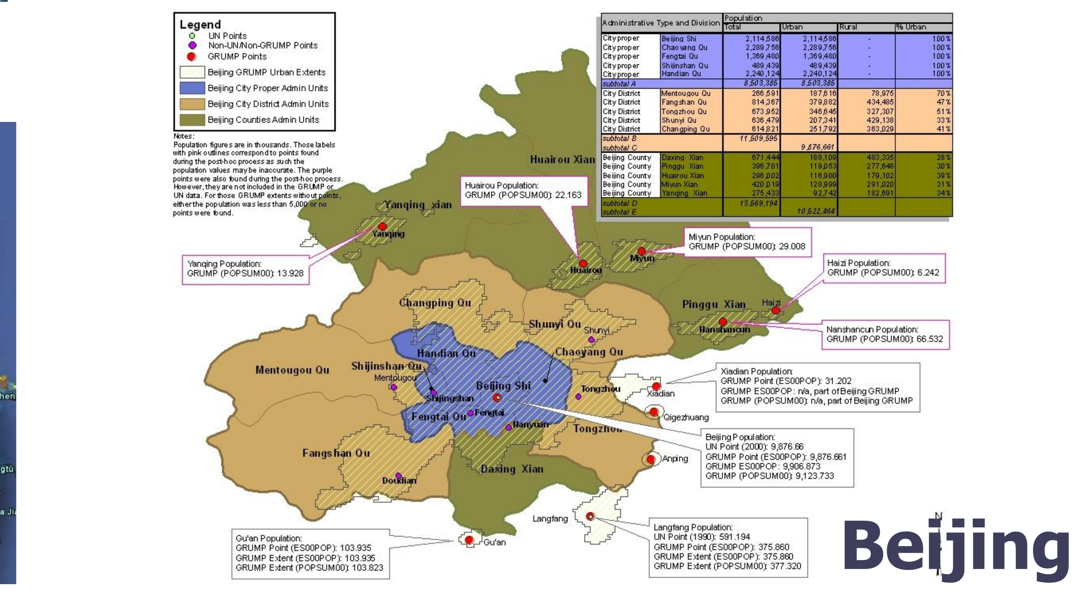


Administrative units and population

## Dense Sampling Method

**Patent Pending US20100280756**

$$P_{Ri} = \frac{P_{Ti}\lambda^2}{(4\pi)^3 R^4} \iint_A dx\,dy\,G(\phi_i, x, y)\,\sigma_0(\phi_i, t_i, x, y)$$

$$P_{Ri} = \frac{P_{Ti}\lambda^2}{(4\pi)^3 R^4}\,\overline{\sigma}_0(\phi_i, t_i) \iint_A dx\,dy\,G(\phi_i, x, y)$$

$$\overline{\sigma}_0(\phi_i, t_i) = \frac{1}{\Gamma_A} \iint_A dx\,dy\,G(\phi_i, x, y)\,\sigma_0(\phi_i, t_i, x, y)$$

$$\overline{\sigma}_0 = \frac{1}{N}\sum_{i=1}^{N}\overline{\sigma}_0(\phi_i, t_i) = \frac{1}{N\Gamma_A}\sum_{i=1}^{N}\iint_A dx\,dy\,G(\phi_i, x, y)\,\sigma_0(\phi_i, t_i, x, y)$$

$$\sigma_0(\phi_i, t_i, x, y) = \overline{\sigma}_0(x, y) + \varepsilon(\phi_i, t_i, x, y)$$

$$\overline{\sigma}_{0M} = \frac{1}{\Gamma_A}\iint_A dx\,dy \left[\sum_{i=1}^{N}\frac{G(\phi_i, x, y)}{N}\right]\overline{\sigma}_0(x, y)$$

$$\mathcal{R} = \frac{1}{\Gamma_A}\iint_A dx\,dy \sum_{i=1}^{N}\left[\frac{G(\phi_i, x, y)}{N}\,\varepsilon(\phi_i, t_i, x, y)\right]$$

## Verification - Príncipe Island

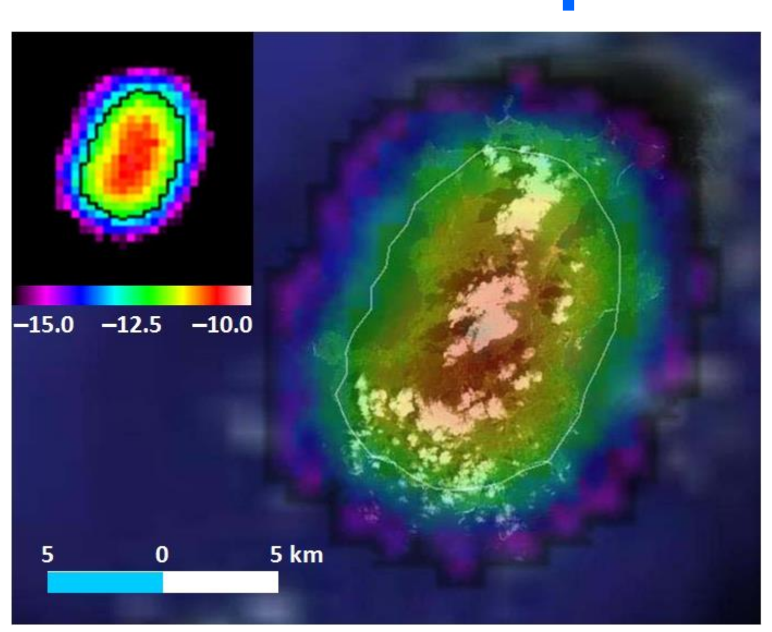


## GATOR-GCMOM Model

**Gas, Aerosol, Transport, Radiation, General Circulation, Mesoscale, and Ocean Model**

1. GATOR-GCMOM is used to simulate the global, regional, and urban climate and air pollution health impacts resulting from urbanization. The goal is to investigate effects on climate and air quality of annual changes in the extent of urbanization over regions of mega urbanization in Asia and to compare with other regions in the 2000s.
2. This model nests climate, meteorological, gas, aerosol, and radiative parameters simultaneously from the global through urban scale. simulates meteorology and its feedback among gases, aerosol particles, cloud hydrometeor particles, surfaces, and radiation. Gas processes include emissions, photochemistry, gas-to-particle conversion, gas-to-hydrometeor conversion and exchange, gas-ocean exchange, advection, convection, molecular diffusion, turbulent diffusion, and dry deposition.
3. At the land surface, each subgrid soil class is divided into vegetated and bare soil. Snow can accumulate on both soil and vegetation. For bare and vegetated soil, the surface energy balance equation accounts for latent heat, sensible heat, solar, thermal-IR, and energy fluxes.
4. Oceans are represented in 3-D for some calculations and 2-D for others. A 2-D time-dependent mixed-layer ocean dynamics model driven by surface wind stress is used to solve for mixed-layer velocities, heights, and horizontal energy transport in each cell. The scheme conserves potential enstrophy, vorticity, energy, and mass and predicts gyres and major currents. Air ocean exchange, vertical diffusion, and 3-D ocean equilibrium chemistry and pH are solved among the Na-Cl-Mg-Ca-K-H-O-Li-Sr-C-S-N-Br-F-B-Si-P system.

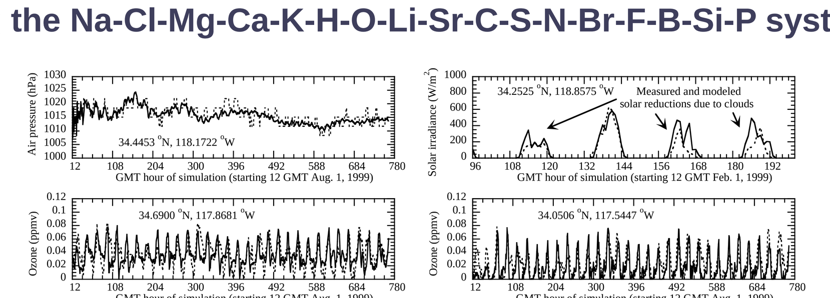

Comparison of modeled with paired-in-time and space air pressure, surface solar radiation, and ozone data [*USEPA*, 2006] at specific locations during August 1999. Model results were from a nested global-through-urban simulation with GATOR-GCMOM

## The Beijing Case Study [Nghiem et al., Encycl. Remote Sens., 2012]

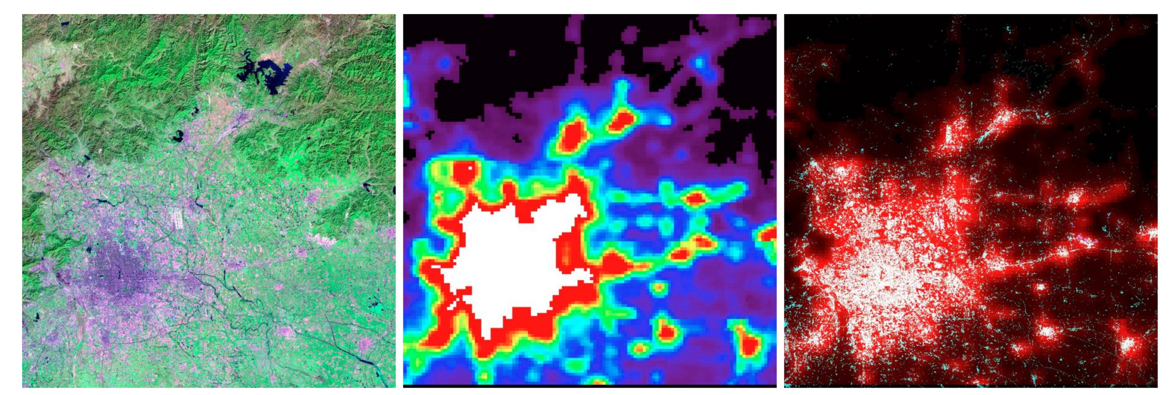

Urban-rural land cover gradients in reflected and emitted light. Landsat 5 false color composite (left) in 2008 show developed, agricultural and undeveloped land cover. Homogeneous green areas are agriculture while the dark pink, purple and gray areas are generally associated with mixtures of SWIR-bright building materials and deep shadow characteristic of more intensive development. Stable night light brightness (center) for 2008 ranges from dim low DN values (purple to cyan) to brighter (green to red) and saturated (white). Unlighted areas (black) are undeveloped. Day-night composites (right) combine Landsat and night lights to illustrate consistencies in land cover and night light brightness. Superimposed night light brightness (red) on upper (green) and lower (blue) bounding estimates of built up extent show high density built environments (white) associated with bright night lights while agriculture and low density rural land cover are associated with lower light levels (DN < ~20).

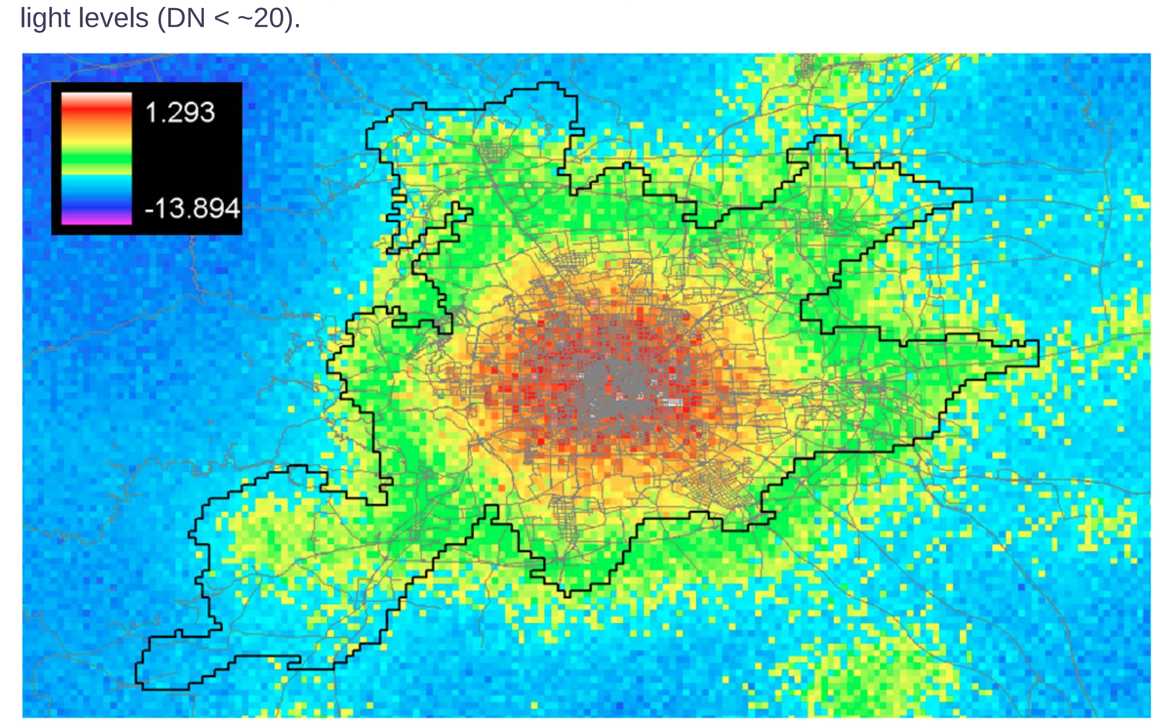


Beijing DSM with road network (grey lines) and Night-Light urban extent (black contour).

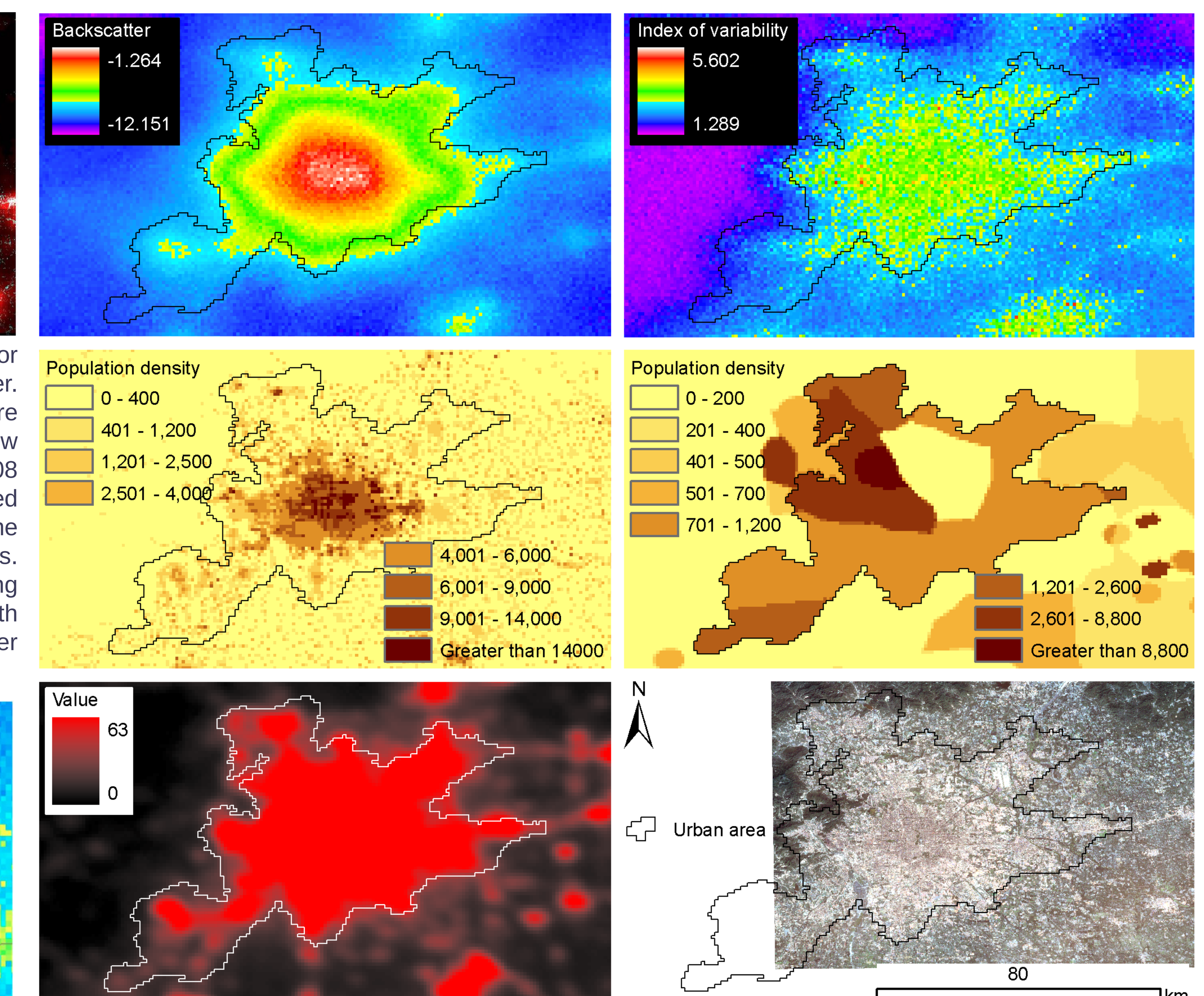


Composite results for Beijing: Top left panel for 2000-2009 DSM average backscatter, top right panel for 2000-2009 DSM IV, middle left panel for average ambient population Pa from LS 2004-2008, middle right panel for residential Pr from GRUMP 2000, bottom left panel for 2000-2009 NL, and bottom right panel for Landsat. NL9495 contour is overlaid on all images as the common reference area.

| Urban area | n (5% cases) | GRUMP 2000 | | LS 2004-2008 | |
|---|---|---|---|---|---|
| | | DSM 00-09 | NL 00-09 | DSM 00-09 | NL 00-09 |
| Beijing | 248 | –0.046 | –0.12 | 0.724 | 0.475 |

**Acknowledgments**

The research carried out by the Jet Propulsion Laboratory, California Institute of Technology, was supported by the NASA Land Cover Land Use Change Program.

Thanks to Gregory Neumann for the processing of 10TB of QuikSCAT data through the Dense Sampling Method.

Road network data for Beijing were available from CloudMade.com at http://downloads.cloudmade.com accessed on 1 July 2010.

**Contact:**
Son.V.Nghiem@jpl.nasa.gov
Telephone: 818-354-2982
Jet Propulsion Laboratory
4800 Oak Grove Dr., 300-235
Pasadena, CA 91109, USA